Bayero Journal of Physics and Mathematical Sciences / Vol. 17, No. 1 / Feb., 2026. ISSN: 1597 – 9342, Online ISSN: 2795 - 3866

BAJOPMAS JOURNAL 17(1): 135 – 145
Printed in Bayero University, Kano - Nigeria.

ELASTIC SCATTERING OF ^{3}He ON ^{6}Li, ^{9}Be, ^{24}Mg and ^{56}Fe USING B3Y-FETAL NUCLEON-NUCLEON EFFECTIVE INTERACTION BASED ON THE OPTICAL POTENTIAL FORMALISM

[1]Dalhatu, M.; [2]Adamu, I.D. and [3]Koki, F.S.
[1]Hydraulic Equipment Development Institute Kano
[2]Physics Department, Bayero University Kano
[3]Physics Department, Bayero University Kano.

ABSTRACT
Despite substantial researches in the elastic scattering reaction involving light-ion nuclei as a projectile, the use of Phenomenological potentials as the component of the optical potential in order to reproduce and investigate nuclear structure and reaction dynamics of the experimental data of ^{3}He nucleus poses considerable challenges. Although the phenomenological potential reproduces experimental data to some extent, however, it faces challenges of parameter ambiguity. This ambiguity emanates from the simultaneous adjustment of multiple parameters such as potential depth, diffuseness and radius, such that fitting to experimental data leads to non-unique solutions with indistinguishable result. These limitations of the phenomenological potential have motivated researchers to search a more robust interaction model capable of reproducing and explaining experimental data, leading to the development and adoption of the microscopic potential which demonstrated a promising reliability in this regard. These motivates the microscopic use of the double folding potential for both the real and imaginary parts of the optical potential, enabling the description of the experimental elastic scattering data most appropriately by reducing the parameter ambiguity through the fixing of radial geometry, significant reduction of number of parameters to the use of only renormalization factors and the potential are directly derived from the nucleon-nucleon interaction. This work uses a full folding approach of the optical potential to analyze the elastic scattering of ^{3}He on ^{6}Li, ^{9}Be, ^{24}Mg and ^{56}Fe nuclei using the DDB3Y nucleon-nucleon effective interaction to obtained the strength of the folded potentials, the reaction cross-section and the total cross-section. The reaction and total cross-section which measures the probability of all non-elastic channel and the overall interaction probability between target and projectile nuclei were obtained for the elastic scattering reaction of ^{3}He on ^{6}Li, ^{9}Be, ^{24}Mg and ^{56}Fe were calculated to be σ_r =709.61 mb $\sigma_T = 1264.43$ mb, σ_r =948.35 mb, $\sigma_T = 1703.54mb$, $\sigma_r = 1010.55\,mb$ $\sigma_T = 1788.95\,mb$ and σ_r =1532.07 mb $\sigma_T = 2654.25mb$ respectively. The cross-sections are analyzed in three regions; the forward angle (0^o –30^o), the intermediate angle (30^o–90^o) and the backward angle ($90^o - 180^o$). At forward angle the scattering is dominated by long range is coulomb interaction and a weak nuclear effect for all the interactions, at the intermediate angle, oscillatory structure is observed which are due to interference between coulomb and nuclear scattering, the oscillations emanated from partial wave interference and Fraunhofer diffraction. At the backward angle, the scattering is dominated by absorption effects, compound nucleus effects. The real potentials were observed to be predominantly attractive at short distances, and as the distance increase the potential was observed to be less attractive which shows that the nuclear force is short-ranged. It was observed that, there is a weak absorption for light nuclei ^{6}Li ^{9}Be and a moderate absorption for medium nuclei and also a strong absorption for heavier nuclei such as ^{56}Fe primarily due to the increasing depth of the imaginary potential associated with higher nuclear density and other reaction channels available. The systematics of the cross-sections have demonstrated the efficacy of

DDB3Y interaction based on the optical model approach in describing and providing explanation of the ^{3}He nucleus scattered from a light, medium and heavy nuclei where the strength of the increases with increase in target mass. The work serves as a tool in providing an alternative way of reducing the parameter ambiguity and a stepstone for future theoretical researches.

Keywords: Optical potential, microscopic potential, phenomenological potential, DDB3Y effective interaction

1.0 INRODUCTION

Elastic scattering involving light-heavy-ion nuclei as projectiles is pivotal in the investigation of nuclear structure and the dynamism of nuclear reaction [1]. Among these light-ion nuclei, the Helium-3 is of significant interest to researchers due its weak binding energy, abundance, internal structure and its sensitivity to both elastic and non-elastic channels during a nuclear interaction [2]. Elastic scattering is a fundamental nuclear reaction where the total kinetic energy and the internal states of the interacting nuclei of the projectile and the target remained unchanged [3]. Researchers have recently put significant effort to search for an appropriate theoretical framework capable of explaining experimental data from elastic scattering reaction [4]. Among these frameworks, Optical potential has been widely used with great success as the most reliable theoretical framework in describing such data [5].

This optical potential is composed of real and imaginary component which represent the elastic and non-elastic channels, respectively [6]. Recently this potential is being constructed by theorist either phenomenologically or microscopically [7]. Although the phenomenological potential reproduces experimental data to some extent, however, it faces challenges of parameter ambiguity [8-12]. This ambiguity emanates from the simultaneous adjustment of multiple parameters such as potential depth diffuseness and radius such that fitting to experimental data leads to non-unique solutions with indistinguishable result [13] This limitations of the phenomenological potential have ever since motivated researchers to search a more robust interaction models capable of reproducing and explaining experimental data, leading to the development and adoption of the microscopic potential which demonstrated a promising reliability in this regard [14-15]. Double-folding potential has been successfully used within a microscopic approach where it is constructed by folding the nucleon-nucleon effective interaction over the density distribution of the interacting nuclei [11]. Different Effective nucleon-nucleon interactions have been used within this approach, including the M3Y and its density dependent versions which were derived from the G-matrix [12]. Recently a modified version of the M3Y has been developed based on the lowest order variational constraints (LOCV) with improved density dependent and agreement with nuclear matter properties [14-15].

In this work a full folding approach is used in which both the real and imaginary components of the optical potential are handled microscopically using the density dependent version of the B3Y-Fetal (DDB3Y) nucleon-nucleon effective interaction. This approach is applied to the elastic scattering of ^{3}He from ^{6}Li, ^{9}Be, ^{24}Mg and ^{56}Fe. The effective nucleon-nucleon interaction is constructed after which the parameters of the DDB3Y and the zero-range pseudo potential are determined using maple software. These parameters are then applied systematically into the NRV code to obtain the strength and folded potential, the magnitude of the reaction and total cross-section. This work provides an improved description of the ^{3}He elastic scattering with a full folding approach which has advantages over the traditional way and also strengthening the link between nuclear structure and reaction observable.

2.0 THEORETICAL FRAMEWORK

The direct and exchange component of of the DDB3Y nucleon-nucleon interactions are express as [14]

$$V_{00}^{D}(r) = \frac{6591.54e^{-4r}}{4r} - \frac{1777.55e^{-25r}}{2.5r}, \quad (1)$$

$$V_{00}^{EX}(r) = \frac{6158.09e^{-4r}}{4r} - \frac{2253.33e^{-25r}}{2.5r} - \frac{7.8474477\, e^{-0.7072}}{0.7072r}, \quad (2)$$

a density dependent form factor is included into the B3Y-Fetal in order to make the nuclear matter saturated rather than collapsing as [16]

$$V_{00}^{D(EX)}(\rho\, r) = F(\rho) V_{00}^{D(EX)}(r), \quad (3)$$

$$\text{where } = F(\rho) = C(1 + \alpha \exp(-\beta\rho)) \quad (4)$$

The parameters of equation (4) were determined through some iterations using maple software thereby evaluating equation (3)

The magnitudes of the direct potential of equation (1) were supplied appropriately into the NRV code.

While the magnitudes of the exchange potential of equation (2) were used to calculate the zero-range pseudo potential using same software as [16]

$$V_E = J(E)\sigma(r) \quad (6)$$

where $J(E)$ is the exchange amplitude

and $\sigma(r)$ is the energy dependence which is given as [17]

$$[1 - \gamma \left[\frac{E}{A}\right] \quad (6i)$$

equation (6i) was used to evaluate equation (6)

then the potential of the target and the projectile is now given as (17)

$$V_{pt} = V_D + V_E \quad (7)$$

where V_E is the exchange potential that was evaluated using equation (6)

2.1 THE DOUBLE FOLDING POTENTIAL

The V_{pt} is then folded with the density distributions of both the projectile and the target as [18]

$$V_F = \iint \rho_p(r_p)\rho_t(r_t)V_{pt}(r_{pt})dr_p dr_t \quad (8)$$

Equation (8) is the double folding potential which was evaluated using equation (7) and (9)

$$\rho_p = \rho_0[1 + \exp\left(\frac{r - R_{p(n)}}{a_{p(n)}}\right)]^{-1} \quad (9)$$

where equation (9) is the two-parameter fermi function [19]

where ρ_0 and $R_{p(n)}$ are the nuclear matter density parameters and $a_{p(n)}$ is the diffuseness parameters.

The neutron (proton) half radii are parameterized as [20]

$$R_p = 0.449 + 0.0071\,(\frac{Z}{N})$$

$$R_n = 0.446 + 0.0072\,(\frac{Z}{N})$$

While the value of ρ_0 is given as

$$\rho_0 = \begin{cases} \int \rho_p\,(r)d^3r = Z \\ \int \rho_n\,(r)d^3r = A - Z \end{cases}$$

The folded potential is then express in terms of nuclear potential as [5]

$$V_N = V_F(N_r + iN_i) \tag{10}$$

N_r is the real renormalization factor N_i is the imaginary renormalization factor.
Here, both the real and imaginary potentials are folded as seen above.
The optical potential is then defined in terms of the coulomb and the nuclear potential as [20]

$$U^{OP} = V_N + V_C \tag{11}$$

where V_C is the coulomb potential and is defined as [21-22]

$$V_C = \begin{cases} \frac{Ze^2}{2R}\left(3 - \frac{R^2}{R_C^2}\right) \; R \leq R_C, \\ \frac{Ze^2}{R} \;\; , R \geq R_C \end{cases}$$

Schoedinger equation then incorporate the optical potential of equation (11) as its central component to account for the relative motion of the interacting nuclei as [23]

given below $$\left[\frac{-\hbar^2}{2\mu}\nabla^2 + U^{OP}\right]\psi(r) = E\psi(r) \tag{12}$$

since the potential here is assumed to be central potential, the intrinsic spins are ignored, the scattering wavefunction is given as

$$\psi(k,R) = \frac{1}{KR}\sum_L^{\infty}(2L+1)^{il}\chi_l(k,r)P_l(\cos\theta) \tag{13}$$

The radial wavefunction $\chi_l(k,r)$ satisfies the radial Schrodinger equation (12) as

$$\left[\frac{\hbar^2}{2\mu}\frac{d^2}{dR^2} - \frac{\hbar^2}{2\mu}\frac{L(L+1)}{R^2} - U(r) + E\right]\chi_l(K,R) = 0 \tag{14}$$

Solving the above equation numerically from R=0 starting from $\chi_l(k,r) = 0$ up to the maximum radius R_{max}. At this distance boundary conditions are imposed such that [24]

$$\chi_l^{(+)}(K,R)|R_{max} = \frac{i}{2}e^{-i2\sigma_l}[H_l^{(-)}(\eta, KR_{max}) - S_l H_l^{+}(\eta, KR_{max})] \tag{15}$$

Where $H_l^{(\pm)}(\eta, KR_{max})$ are the outgoing and ingoing coulomb function and σ_l is the coulomb shift and S_l is the scattering matrix element. Using equation (15) the coefficient of the s-matrix element is determine which are then used to obtain the scattering amplitude of equation (16)
The scattering amplitude was calculated as [25]

$$f(\theta) = f_c(\theta) + \frac{1}{2ik}\sum_l(2l+1)e^{2i\delta l}(S_l - 1)P_l(\cos\theta) \tag{16}$$

where $f_c(\theta)$ is the coulomb scattering amplitude
The elastic differential cross-section was expressed as

$$\frac{d\sigma}{d\Omega}(\theta) = |f_c(\theta) + f_N(\theta)|^2 \tag{17}$$

While the elastic and reaction cross-sections were respectively expressed as

$$\sigma_{el} = 2\pi\int_0^{\pi}|f(\theta)|^2\sin\theta d\theta = \frac{\pi}{K^2}\sum_{l=0}(2l+1)|S_l - 1|^2 \tag{18}$$

and

$$\sigma_r = 2\pi\int Jds = \frac{\pi}{K^2}\sum_{l=0}(2l+1)(1 - |S_l|^2 \tag{19}$$

The total scattering cross-section is defined as

$$\sigma_{tot} = \sigma_{el} + \sigma_r = \int d\Omega \frac{d\sigma}{d\Omega}(\theta) = \frac{\pi}{k^2}\sum_{l=0}^{\infty}(2l+1)|S_l - 1|^2 \qquad (20)$$

3.0 PROCEDURE

The parameters of the density dependent version of the B3Y-Fetal effective interaction are determined by solving two equations simultaneously and also using the parameters of the exchange potential of the effective interaction to determine the zero-range pseudo potential using maple software 2023. Then the above determined parameters together with those of the direct potential are taken as input systematically into the folding model of the NRV code where an option of custom is provided in order to have a unique interaction. The density of both the projectile and target was taken from the two fermi-parameter function. EXFOR software (which is from Hokkaido University Nuclear Reaction Data center, last updated, 28th February, 2026) was then used to obtain experimental data, (the data was obtained from a published paper within the EXFOR software) by specifying the projectile, target, quantity (partial differential data with respect to angle, differential data with respect to angle among others), Emission (elastic scattering, inelastic scattering, transfer reaction among others). Collision energy was obtained from this experimental data. The data is then input into the NRV code in order to solve the Schrödinger equation using optical code and finally the theoretical calculations was compared with the obtained experimental data graphically. R_{max}, l_{max} and dR are integration parameters were chosen appropriately in order to numerically solve the Schrödinger equation. The calculate button was then pressed where an output file was obtained which is graphical and text form. The renormalization constants were varied in order to obtain the best fit between experimental data and theoretical calculations. Total cross-section, reaction cross -section plot and the differential cross-section were simultaneously obtained. The process was repeated for different nuclei at different energies.

4.0 RESULT AND DISCUSSIONS

4.1 RESULTS

The results of the elastic scattering reaction of ^{3}He from ^{6}Li, ^{9}Be, ^{24}Mg and ^{56}Fe are displayed graphically and in a tabular form as given below. The elastic scattering analyses of ^{3}He from ^{6}Li, ^{9}Be, ^{24}Mg and ^{56}Fe were carried out at different energies using the B3Y-Fetal effective Interaction within the frame work of optical potential. The Strength of the component of the real and imaginary of the folded potential were determined using the double folding model. Renormalization constants were appropriately used for proper fitting. The reaction cross section the total cross section and other reaction parameters were determined as shown in table 1 below. Furthermore differential cross-section and strength of the folded potential were also obtained as shown in the figures below.

Table 1 represent the reactions kinematics

Targets	Elab (Mev)	N_r	N_i	$k\,fm^{-1}$	η	σ_r	σ_T
^{6}Li	60	0.9	0.64	1.956	0.211	709.61	1264.43
^{9}Be	50	1.3	0.8	2.009	0.309	948.35	1703.54
^{24}Mg	130	0.7	0.64	3.839	0.574	1010.55	1788.95
^{56}Fe	33.45	1.02	1.0	2.079	2.452	1532.07	2654.25

The determined the reaction and total cross-section and the reaction kinematics were reported in table 1 above.

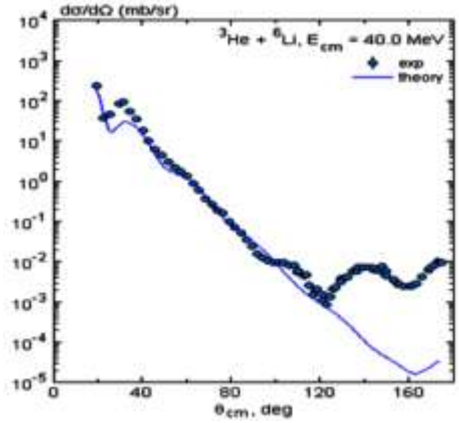

Fig 1. Angular distribution of ^{3}He+ ^{6}Li elastically scattered at Elab = 60Mev

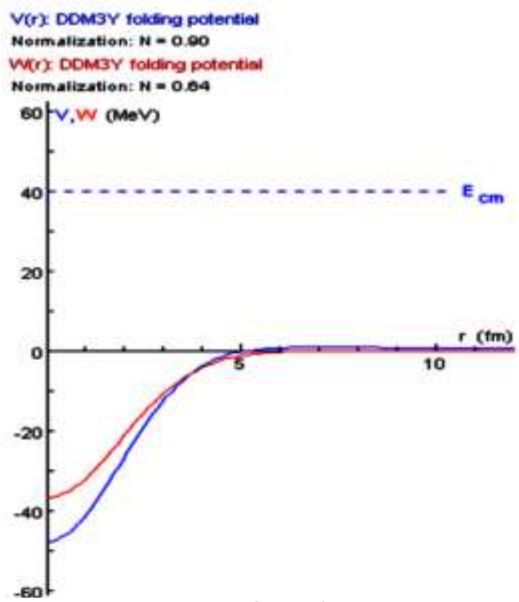

Fig 2. The depth of the folded potential ^{3}He+ ^{6}Li elastic scattering at Elab = 60Mev

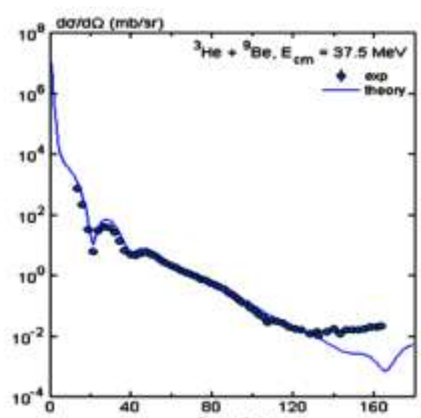

Fig 3 Angular distribution of ^{3}He+ ^{9}Be elastically scattered at Elab = 50Mev

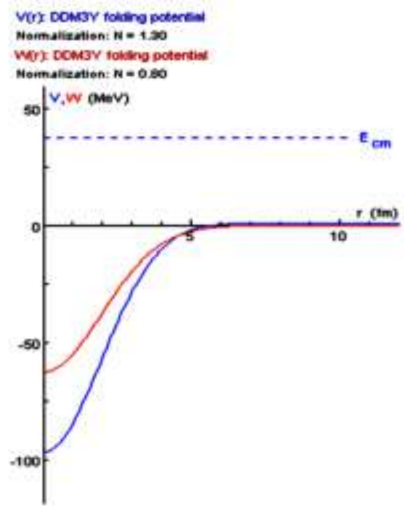

Fig 4. Strength of the folded potential ^{3}He+ ^{9}Be elastically scattered at Elab = 50Mev

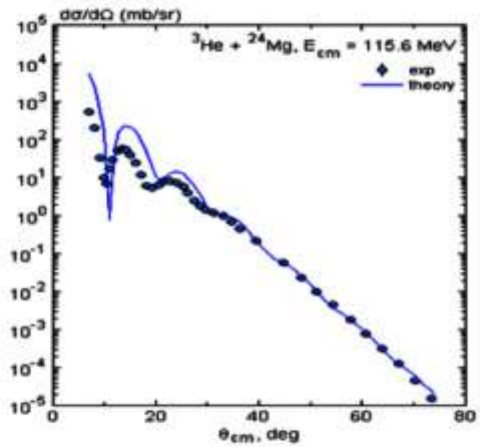

Fig 5 Angular distribution of ^{3}He+ ^{24}Mg elastically scattered at Elab = 130Mev

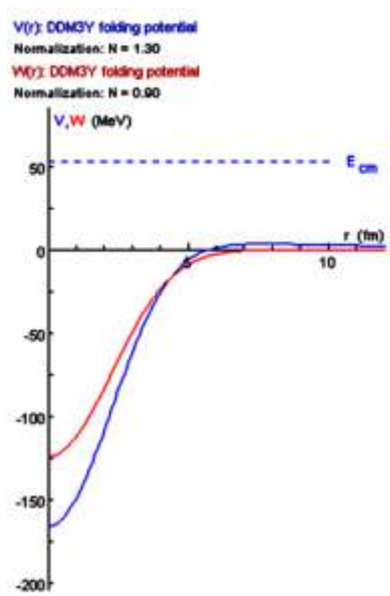

Fig 6. Strength of the folded potential of ^{3}He+ ^{24}Mg elastically scattered at Elab = 130Mev

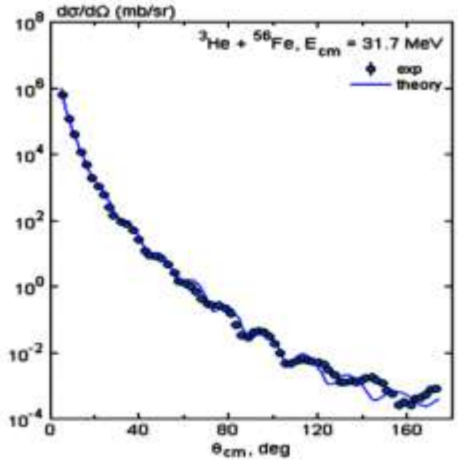

Fig. 7. Angular distribution of ^{3}He+ ^{56}Fe elastically scattered at Elab = 33.45Mev

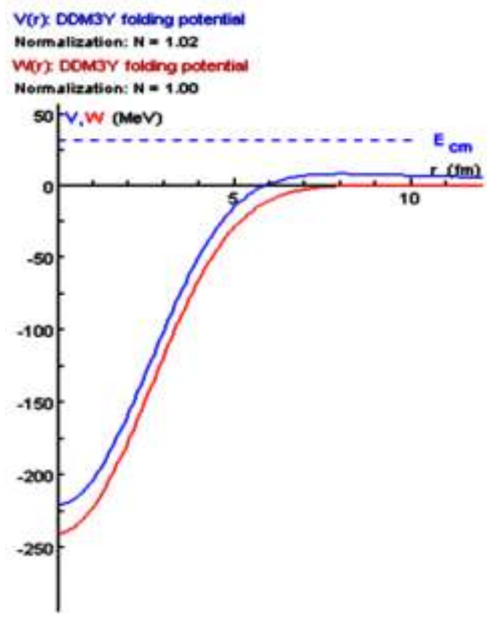

Fig. 8. Strength of the folded potential of ^{3}He+ ^{56}Fe elastically scattered at Elab = 33.45 Mev

4.2 DISCUSSIONS

Figures 1,3,5 and 7 represent Represents the differential cross-section as a function of center of mas scattering angles of (^{3}**He)** from ^{6}Li ^{9}Be ^{24}Mg and ^{56}Fe.The dotted lines represent the experimental data (published work) while the solid lines represent the theoretical calculations. The cross-sections are analyzed based on three regions; the forward angle ($0^{\circ} - 30^{o}$), the intermediate angle ($30^{o} - 90^{\circ}$) and the backward angle ($90^{\circ} - 180^{\circ}$). At forward angle the scattering is dominated by long range is coulomb interaction and a weak nuclear effect for all the interactions, so the compound nucleus contribution is negligible due small time of interaction and also the pre-equilibrium effects are minimal because the reaction is yet to proceed beyond initial interaction. At the intermediate angle, oscillatory structure is observed which are due to interference between coulomb and nuclear scattering, the oscillations emanated from partial wave interference and Fraunhofer diffraction, in this region there is weak compound contribution and the pre-equilibrium effects has started emanating through partial loss of flux in the elastic channel and redistribution of energy. At the backward angle, the scattering is dominated by absorption effects, compound nucleus effects. Compound systems are formed but weak for the ^{56}Fe nucleus and there is reasonable condition pre-equilibrium contribution especially for^{6}Li ^{9}Be nuclei. Conclusively, the theoretical curve generally aligns with the experimental data and also with its oscillatory structure especially at the forward and intermediate angles especially for ^{24}Mg and ^{56}Fe. This shows that the theoretical model was able to describe the elastic scattering mechanism. And also, there is an excellent fit between experiment and theory, which demonstrate the effectiveness of the optical potential using the DDB3Y. Figures 2,4,6 and 8 represent the Represent the depth of the folded potential as a function of the radial distance (r) while the Y-axis represent the potential depth in Mev while the X-axis with a dashed line represents the center of mass energy of (**^{3}He**) on ^{6}Li ^{9}Be ^{24}Mg and ^{56}Fe. The blue solid lines represent the real folded potential while the solid red line represent the imaginary potential. The real potentials were observed to be predominantly attractive at short distances, and as the distance increase the potential becomes less attractive which shows that the nuclear force is short -ranged. The imaginary part of the potential account for the absorption flux from the elastic scattering channel into other non-elastic reaction channels. It was observed that, there is a weak absorption for light nuclei ^{6}Li ^{9}Be and a moderate absorption for medium nuclei and also a strong absorption for heavier nuclei such as ^{56}Fe primarily due to the increasing depth of the imaginary potential associated with higher nuclear density and other reaction channels available.

5.0 CONCLUSION

This work presents a detailed analysis of elastic scattering of Helium-3 (**^{3}He**) on ^{6}Li ^{9}Be ^{24}Mg and ^{56}Fe was carried out using the DDB3Y-Fetal nucleon-nucleon effective interaction. Double folding potential was used both as the real and imaginary component of the optical potential. The work addresses the limitation of parameter ambiguity of the phenomenological potential through the use of double folding potential. The cross-sections are analyzed based on three regions; the forward angle ($0^{\circ} - 30^{o}$), the intermediate angle ($30^{o} - 90^{\circ}$) and the backward angle ($90^{\circ} - 180^{\circ}$).

At forward angle the scattering is dominated by long range is coulomb interaction and a weak nuclear effect for all the interactions, so the compound nucleus contribution is negligible due small time of interaction and also the pre-equilibrium effects are minimal because the reaction is yet to proceed beyond initial interaction. At the intermediate angle, oscillatory structure is observed which are due to interference between coulomb and nuclear scattering, the oscillations emanated from partial wave interference and Fraunhofer diffraction, in this region there is weak compound contribution and the pre-equilibrium effects has started emanating through partial loss of flux in the elastic channel and redistribution of energy. At the backward angle, the scattering is dominated by absorption effects, compound nucleus effects. Compound systems are formed but weak for the ^{56}Fe nucleus and there is reasonable condition pre-equilibrium contribution especially for^{6}Li ^{9}Be nuclei. The real potentials were observed to be predominantly attractive at short distances, and as the distance increase the potential becomes less attractive which shows that the nuclear force is short -ranged. The imaginary part of the potential account for the absorption flux from the elastic scattering channel into other non-elastic reaction channels. It was observed that, there is a weak absorption for light nuclei ^{6}Li ^{9}Be and a moderate absorption for medium nuclei and also a strong absorption for heavier nuclei such as ^{56}Fe primarily due to the increasing depth of the imaginary potential associated with higher nuclear density and other reaction channels available. The obtained result of ^{3}He induced reaction cross section is pertinent in the production of medical and industry isotopes. ^{3}He are increasingly used in cyclotron-based isotope production, particularly for positron-emitting radionuclides and theranostic isotope.it also has significant importance for nuclear data evaluation in support of accelerator-based technologies including neutron source design, material irradiation studies and space radiation shielding. The above analysis indicates that, the double folding potential provides a coherent description of the ^{3}He elastic scattering from light to heavy and also in its capacity to reproduce the angular distribution of the experimental data. The result shows the applicability of the DDB3Y in exploring the nuclear structure and reaction dynamics of ^{3}He induced reaction. This work can be extended to predict cross-section for ^{3}Heinduced reactions such as transfer and breakup reaction for a unified description of the reaction. It is also recommended to carry out this reaction using unstable target nuclei, higher incident energy, coupled-channels analyses which will further strengthen the capability of the double folding model.

REFERENCES

[1] M. E. Kurkcouglu, H. Ayterkin and I. Boztousan "Optical model analysis of the ^{16}O+ ^{16}O Nuclear scattering reaction around Elab=5 Mev/Nucleon", *G.U journal of science*, 19(2) 105-112, 2006.

[2] M.N. El-Hammany, "Double folding analysis of ^{3}He elastic and inelastic scattering to low lying states on ^{90}Zr, ^{116}Sn and ^{208}Pb at 270 Mev", *Chinese Physics C*, vol. 39, n0. 3 034101, 2015.

[3] M. Aygun, O. Kocadag and Y. Sahin, "Phenomenological and Microscopic model analysis of elastic scattering reactions of ^{18}O by ^{24}Mg, ^{28}Si, ^{58}Ni ^{64}Zn, ^{90}Zr, ^{120}Sn and ^{208}Pb target Nuclei", *Revista Mexicana de Fisca,* 61, 414-420, 2015.

[4] R.C. Abenga, and J. Fiase, "Elastic scattering of ^{12}C+ ^{12}C and ^{16}O+ ^{16}O using an effective mass dependent M3Y-Type Interaction", *International journal of Innovative Research and Advanced Studies (IJIRAS)* Vol. 6, Issue 2, 2019.

[5] R.C. Abenga, Y.Y. Ibrahim and K.L. Ibrahim, "Strong Absorption and the Double folding Potential using B3Y-Fetal Interaction", *Caliphate Journal of science and Technology*, ISSN -313X ,2024.

[6] A.J. Kohing, J.P Delaroche "Local and Global Nuclear Optical model from 1Kev to 200 Mev" *Nuclear Physics A,* 713, 231-310, 2003.

[7] I. Ochala, "Optical Model Analysis of elastic scattering of ^{12}O+ ^{12}C", *International Journal of Applied Mathematics and Theoretical Physics*, 7(1): 1-9, 2021.

[8] Z. Gao-Long, Z. Huan-Quio, L. Zu-Hua, Z. Chun-Lei, L. Cheng, J.Y. Fang, A. Guang-Peng, J. Hui-Ming, W. Zhen-Deng, X. X. Xing, B. Chun-Lin and Y. Ning, "Double Folding Calculation applied to the real part of the Interacting potential", *High energy Physics and Nuclear Physics,* Vol. 31, No. 7, 2007.

[9] V.K. Lukyanov, D.N. Kadrev, E.V. Zemalyanaya, A.N. Antonov, K.V. Lukyanov and M.K. Gaidarov, "^{4}He+ ^{12}C elastic scattering using a Microscopic Optical Potential", *Physical Review C Nuclear Physics* 82 (2), 024604.

[10] A.H. Amer, A. Amar, Sh. Hamada, I.I. Bondouk and F.A. El-Husainiy, "Optical and Double Folding Model Analysis for Alpha Particles Elastically Scattered from ^{9}Be and ^{11}B At Different Nuclear Energies" *International Journal of Chemical and Molecular Engineering,* Vol. 10 No. 2, 2016.

[11] M. Aygun, "A microscopic analysis of elastic scattering of ^{8}Li Nucleus on different target Nuclei", *Acta Physica Polonica B,* No.9,

[12] K. Hagino, T. Takechi and N. Takagiwa, "No recoil approximation to knock-on exchange potential in the double folding model for heavy-ion collisions" 2018

[13] C.D Prutt, J.E. Escher and R. Rahman, "Uncertainty Quantified phenomenological optical potential for single-nucleon scattering", *Physical Review* C 107, 014602, 2023.

[14] D.T. Khao, G.R. Satchler, "Generalized Folding Model for the Elastic and Inelastic Nucleus-Nucleus Scattering Using Elastic Density Dependent Nucleon-Nucleon Interaction", *Nuclear Physics A* 668, 3-41, 2000.

[15] J.O. Faise and K.R.S. Daven, "Mass dependent of M3Y-type interaction and the effects of tensor correlations", *Physical Review C* 66 014004, 2002.

[16] I. Ochala, J.O.Fiase, "Symmetric Nuclear Matter Calculation Variational Approach", *Physcial Review C* 98 064001, 2018.

[17] M Modarres and M. Rahmat, "The LOCV averaged two-nucleon Interactions versus the Density Dependent M3Y Potential for the Heavy-ion Collisions", *Nuclear Physics A*, 934, 148-166 2015.

[18] M.E. Brandan and G.R. Satchler, "The interaction between light heavy-ions and what tell us" Physics reports 143-243,1997

[19] Z. Gao-long, L. Hao and L. Xiao-Yun, "Nucleon-nucleon interaction in the double folding model for fusion reaction", Chinese Physics B, Vol. 18, No.1 1674-1056, 2009.

[20] S.D. Olorunmi and A.S. Olatinwo, "Analysis of elastic scattering cross-section of ^{16}O on ^{27}Al and ^{154}Sm using semi-Microscopic double folding model"*Ife journal of scienc, Vol 25, No. 2,* 2023.

[21] A.M. Khalaf, M.M Khalifa, A.H.M. Solieman and M.H.N. Comsan, "Nuclear matter parameter and Optical model Analysis of proton scattering on the doubly magic Nucleus" *Nuclear physics A*, 2017.

[22] Y. Li-Xu, "Applicability of the systematic ^{3}He potential for triton nucleus reaction", Journal of Modern Physics E, Vol. 24, No. 1, 2015

[23] Y. Pelagi, R. Pnini, and E. Zaarur, "Quantum mechanics" 1998, ISBN 0-07-054018-7, McGraw-Hill companies inc.

[24] Noureddine Z. "Quantum mechanics, concept and applications", second edition, 2009 john whiley and sons Ltd.

[25] G.R Satchler, "Direct Nuclear reactions", Oxford university press, Wallen street oxford, ISBN 0-19-851269-4, 1983.